all in its absence, even at higher temperature.[14] The ^{1}H NMR spectrum of this complex revealed an unusually shielded resonance for the central proton, greater than 1.1 ppm upfield from that in the kinetic isomer, and significantly deshielded resonances for the terminal protons.[13] In addition, the thermodynamic product **2b** showed well-resolved second-order multiplets for the ethylene ligand, contrasting the fluxionally broadened resonances seen at room temperature in kinetic product **2a**. Diffractable single crystals of complex **2b** were obtained from acetone/ether, and the configurational assignment was confirmed by X-ray crystallography, rigorously establishing the endo allyl orientation in the thermodynamic product (Figure 2).[11] Perhaps most interestingly, photolysis of the endo isomer **2b** in acetone under 30–60 psi of ethylene established a photostationary equilibrium favoring the less stable exo isomer in a ratio of ca. 10:1 (eq 2).[15]

In marked contrast to the unsubstituted allyl complex **2a**, the reaction of exo crotyl complex **3a** with Ph$_3$P resulted in clean substitution of the ethylene, giving the crotyl phosphine complex **6** in 71% isolated yield after purification (Scheme II).[10,16] Also in contrast to the reactivity of complex **2a**, thermal isomerization to the endo complex **3b**[14] is obtained between 60 and 100 °C in the absence of catalyst. Although not required, this isomerization is best conducted under ethylene, inhibiting decomposition from competitive ligand dissociation. The substitutional lability and facile thermal isomerization observed for the crotyl complex may indicate that ligand substitution in this complex follows an associative pathway, preceded by η^3 to η^1 isomerization of the allyl ligand to open a coordination site at the metal. Such dissociation is expected to be more facile for the substituted allyl ligand, with its weaker secondary carbon–metal interaction, than for the unsubstituted allyl ligand. This suggests that a fundamentally different mechanism is operative in the phosphine-catalyzed isomerization of unsubstituted complex **2a**. This process is under investigation.

While the kinetic selectivity for the less stable exo allyl isomers is difficult to rationalize, the use of ethylene indeed enables allylic activation to proceed for more highly substituted olefins, consuming only 1 equiv of the substrate olefin. Importantly, this methodology provides ready access to "polyfunctional" organometallic electrophiles (both the ethylene and two sites of the allyl ligand are potentially subject to nucleophilic attack[1d]) and both geometries of the allyl ligand, allowing a detailed investigation of nucleophilic addition in this system. Development of other potentially "enabling" ligands and extension of this methodology to complexes of other metals and to more highly substituted, cyclic, and functionalized olefins is also under investigation.

Acknowledgment. We thank Dr. John C. Huffman and Kirsten Folting of the Indiana University Molecular Structure Center for the X-ray crystal structure determinations and the Union Carbide Innovation Recognition Program for financial assistance.

Supplementary Material Available: Spectroscopic and analytical data for compounds **3a**, **3b**, and **4–6**, details of the data collection and structure solution for complexes **2b** and **3a**, and tables of atomic positional and thermal parameters and complete bond distance and angle data for **2b** and **3a** (30 pages); listings of F_o vs F_c for **2b** and **3a** (14 pages). Ordering information is given on any current masthead page.

---

(14) (a) Exo–endo allyl isomerization catalyzed by nucleophiles has been described: Faller, J. W.; Chao, K. H.; Murray, H. H. *Organometallics* **1984**, *3*, 1231 and references therein. VanArsdale, W. E.; Winter, R. E. K.; Kochi, J. K. Organometallics 1986, 5, 645. (b) Exo and endo allyl isomers are known in several systems; see: Hsu, L.,-Y.; Nordman, C. E.; Gibson, D. H.; Hsu, W.-L. *Organometallics* **1989**, *8*, 241. Krivykh, V. V.; Gusev, O. V.; Petrovskii, P. V.; Rybinskaya, M. I. *J. Organomet. Chem.* **1989**, *366*, 129. See also ref 3b, and references therein.

(15) (a) Erker, G.; Berg, K.; Krüger, C.; Müller, G.; Angermund, K.; Benn, R.; Schroth, G. *Angew. Chem., Int. Ed. Engl.* **1984**, *23*, 455. (b) Irradiation for 0.5 h, 450-W Hanovia lamp, Pyrex filter. In the absence of ethylene some photolytic decomposition of these complexes is observed.

(16) The ^{1}H NMR spectrum of the allyl ligand in complex **6** is closely analogous to that reported for Cp*(PMe$_3$)Ir(allyl)$^+$BF$_4^-$,[1b] but because the allyl configuration in that complex has not been unambiguously assigned, the configuration in complex **6** also remains ambiguous.

Articles

π-Complexes of Alkenes to Trivalent Aluminum

Jean Chey, Hyoun-Sook Choe, Yuh-Min Chook, Elke Jensen, Pamela R. Seida, and
Michelle Miller Francl*

Department of Chemistry, Bryn Mawr College, Bryn Mawr, Pennsylvania 19010

Received December 8, 1989

The structures of simple π-complexes of aluminum alkyls and aluminum alkyl halides were explored with use of ab initio molecular orbital theory. Such structures have been proposed as either intermediates or transition structures in mechanisms for oligomerization of ethylene, carbalumination, and hydroalumination. Complexes of AlR$_{3-n}$Cl$_n$ (R = H, CH$_3$) with ethylene and propene were found to be stable intermediates, not transition structures. The energies of binding have been estimated by using post-Hartree–Fock techniques.

The Lewis acidity of trivalent aluminum complexes has been both a blessing and a curse. The ability of the empty aluminum p orbital to accept an electron pair is the root of much of the rich chemistry of aluminum. On the other hand, a great deal of the early work in organometallic chemistry, e.g. the development of the Grignard reagent,

Scheme I

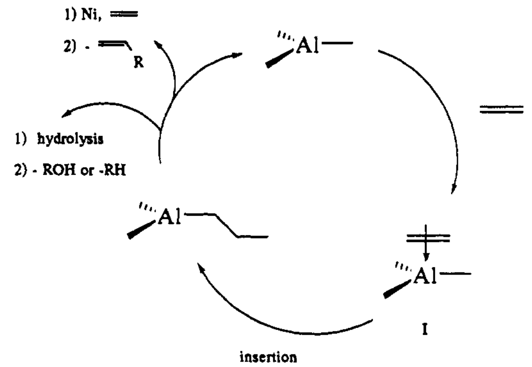

was performed in ether solvents. The strong binding of these solvents to aluminum complexes retarded both their reactivity and the development of the field. It was not until Ziegler's work[1] in the 1950's that organoaluminum compounds began to take their place as reagents in organic synthesis. For example, trialkylaluminum complexes are used in industry to produce long-chain α-olefins and primary alcohols from ethylene

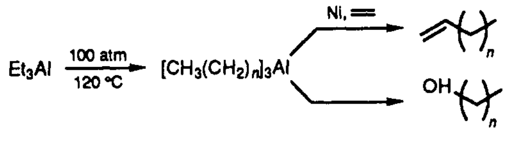

$3 < n < 40$

and in synthetic applications to construct new CC and CH linkages via carbalumination and hydroalumination

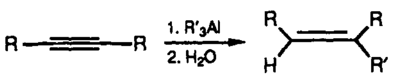

In both these cases the reactive metal species is thought to be the monomeric, as opposed to the generally more stable bridged dimeric, aluminum complex. Scheme I depicts a general pathway for reaction of a multiple bond with an alkylaluminum monomer. The structure of I, which presumably results from electrophilic attack by the aluminum on the π-bond,[2] has been proposed to correspond to either a transition state or a reactive intermediate on the potential energy surface for the reaction. This work will focus on the structural characterization of I and on assessment of its position on the reaction pathway relative to the reactants.

Table I. Selected Hartree–Fock Optimized Parameters[a] for Monomeric Aluminum Alkyl and Alkyl Halide Structures

molecule	pt group[b]	param	HF/3-21G$^{(*)}$	HF/6-31G*	expt
AlH_3	D_{3h}	r(AlH)	1.587	1.584[c]	
$Al(CH_3)_3$	C_1	r(AlC)	1.981[d,g]	1.981[g]	1.964[e]
$AlCl_3$	D_{3h}	r(AlCl)	2.075[f]	2.077	2.06[f]
$AlCl(CH_3)_2$	C_{2v}	r(AlCl)	2.126		
		r(AlC)	1.963		
		∠(CAlC)	126.0		
$AlCl_2CH_3$	C_{2v}	r(AlCl)	2.098		
		r(AlC)	1.948		
		∠(ClAlCl)	116.4		

[a] Bond lengths are in Å and bond angles in degrees. Complete structures and total energies are given in the supplementary material. [b] Symmetry constrained to point group noted. Minimum energy structures were confirmed by normal-mode analysis for AlH_3, $Al(CH_3)_3$, and $AlCl_3$ at 3-21G$^{(*)}$. [c] Reported as 1.587 Å in ref 11b; total energy for structure reported in this work is lower. [d] The AlC bond length only is reported in ref 15. [e] Experimental data from electron diffraction: Almenningen, A.; Halvorsen, S.; Haaland, A. *J. Chem. Soc. D* **1969**, 644. [f] See ref 15. [g] Average value.

Simple π-complexes of trivalent aluminum alkyl halides have not yet been structurally characterized experimentally,[3] but support for them is strong. Alkenylaluminum complexes, $Al[(CH_2)_n(H)C{=}CH_2]_3$ (n = 3, 4), are known to be monomeric in hydrocarbon solutions, while the corresponding alkyl complexes are not.[4] Spectroscopic studies of the $n = 4$ compounds also have revealed a downshift of 22 cm^{-1} in the C═C stretch and deshielding of the vinylic protons in the NMR spectrum.[5] These data suggest that the π-bond is complexed to the metal center, i.e.

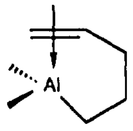

The structure of the unsymmetrically bridged alkynylaluminum dimers[6]

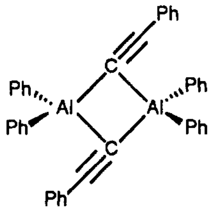

has frequently been put forth as further evidence for π-complexation to aluminum. We[7] and others,[8] however, believe that these are not good models for alkene complexation to trialkylaluminum complexes and may not even be such for the binding of alkynes to aluminum monomers.

We have applied the techniques of ab initio molecular orbital theory to the exploration of the structures of alkene complexes with aluminum alkyls and alkyl halides in order to gain a better understanding of the nature of the proposed intermediate (I). Optimized structures of ethylene complexes of $R_nCl_{3-n}Al$ (n = 1–3; R = H, Me) were determined; normal-mode analyses were performed subsequently to characterize the critical points as either transition structures or minima. Structures were also found for propene complexed to AlH_3. The binding energies for these systems were computed. We discuss below the nature of the bonding between aluminum and carbon and the effect of substitution at the metal on this interaction.

---

(1) Eisch, J. J. In *Comprehensive Organometallic Chemistry*; Wilkinson, G., Stone, F. G. A., Abel, E. W., Eds.; Pergamon: Oxford, U.K., 1982; Chapter 6.

(2) Dolzine, T. W.; St. Denis, J.; Oliver, J. P. *J. Am. Chem. Soc.* **1972**, *94*, 8260.

(3) The analogous complex between aluminum atoms and ethylene has been studied with use of ESR spectroscopy (Kasai, P. H. *J. Am. Chem. Soc.* **1982**, *104*, 1165. Howard, J. A.; Mile, B.; Tse, J. S.; Morris, H. *J. Chem. Soc., Faraday Trans. 1* **1987**, *83*, 3701) and IR spectroscopy (Manceron, L.; Andrews, L. *J. Phys. Chem.* **1989**, *93*, 2964). Theoretical studies (Tse, J. S.; Morris, H. *J. Chem. Soc., Chem. Commun.* **1989**, *78*. Trenary, M.; Casida, M. E.; Brooks, B. R.; Schaefer, H. F., III. *J. Am. Chem. Soc.* **1985**, *107*, 4451. Sakai, S.; Morokuma, K. *J. Phys. Chem.* **1987**, *91*, 3361. Schaefer, H. F., III. *J. Am. Chem. Soc.* **1990**, *112*, 517) suggest these are also symmetric π-complexes.

(4) Dolzine, T. W.; Oliver, J. P. *J. Am. Chem. Soc.* **1974**, *96*, 1757.

(5) Hata, G. *Chem. Commun.* **1968**, 7.

(6) Stucky, G. J.; McPherson, A. M.; Rhine, W. E.; Eisch, J. J.; Considine, J. L. *J. Am. Chem. Soc.* **1974**, *96*, 1941. Jutzi, P. *Adv. Organomet. Chem.* **1986**, *26*, 217.

(7) Seida, P. R.; Wilson, J.; Francl, M. M. Manuscript in preparation.

(8) Pavan Kumar, P. N. V.; Jemmis, E. D. *J. Am. Chem. Soc.* **1988**, *110*, 125.

Table II. Comparison of Theoretical and Experimental Parameters[a] for Aluminum Alkyl and Aluminum Halide Bridged Dimers

molecule	param	HF/3-21G$^{(*)}$	HF/6-31G*	expt
$(AlH_3)_2$[b]	$r(AlAl)$	2.618	2.639	2.62
	$r(AlH_{br})$	1.740	1.747	1.67
	$\angle(AlH_{br}Al)$	97.5	98.0	103
$[Al(CH_3)_3]_2$[c]	$r(AlAl)$	2.622	2.646	2.619
	$r(AlC_{br})$	2.170	2.178	2.140
	$r(AlC_t)$	1.985	1.986	1.957
	$\angle(AlC_{br}Al)$	74.4	74.8	75.5
$(AlCl_3)_2$[c]	$r(AlAl)$	3.255	3.262	3.25
	$r(AlCl_{br})$	2.282	2.289	2.24
	$r(AlCl_t)$	2.079	2.083	2.04
	$\angle(AlClAl)$	90.9	89.1	

[a] Bond lengths are in Å and bond angles in degrees. Complete structures and total energies are given in the supplementary material. [b] Experimental parameters are for $[AlH(CH_3)_2]_2$: Andersen, X.; Almenningen, A.; Forgaard, Z.; Haaland, A. *J. Chem. Soc. D* **1971**, 480. [c] Experimental parameters from reference *e* in Table I.

The significance of these results with respect to the plausibility of the proposed mechanism and the regioselectivity of the reaction is briefly discussed.

Methods

The GAUSSIAN 82 suite of programs[9] was used to perform all electron ab initio molecular orbital calculations. Hartree–Fock energies and optimized structures were determined with use of the 3-21G$^{(*)}$,[10] 6-31G*,[11] and 6-31+G*[12] basis sets. No symmetry constraints were imposed unless otherwise noted in the tables. Normal-mode analyses were performed on the 3-21G$^{(*)}$ structures. Selected molecules were optimized with use of post-Hartree–Fock methods, i.e. MP2/6-31G*. Binding energies were calculated with use of MP2/6-31G*//MP2/6-31G* values whenever feasible. Single points at MP2/6-31G*//HF/6-31G*, MP2/6-31+G*//HF/6-31G*, or MP2/6-311+G*//HF/6-31G* were used otherwise. Charge density difference plots from CDIFF82[13] and molecular orbital plots[14] were employed to analyze the bonding.

Results and Discussion

A. Structures. We initially found optimized structures for the monomeric aluminum alkyls and alkyl halides given in Table I. While all were constrained to be planar, 3-21G$^{(*)}$ normal-mode analyses of the three R_3Al (R = H, Cl, CH_3) molecules confirm that the planar structures are minima on the potential energy surface. The 3-21G$^{(*)}$ and 6-31G* basis sets yield very similar structures, as has been noted in the past.[15] The largest deviation in bond lengths between the two basis sets in this study is less than 0.005 Å. Theoretically determined parameters compare favorably with those from experiment in the two cases for which data are available.

Many aluminum alkyls and alkyl halides exist not as monomers but as bridged dimers, e.g.

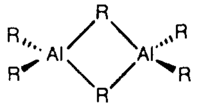

Optimized structures for some dimers are compared with experimental data in Table II. Again, the Hartree–Fock models perform capably. The deviations in bond length from experiment at 6-31G* are generally less than 0.05 Å, and the structure of the bridge is well reproduced. The only case for which the 6-31G* structure of the bridge is poor is the AlH_3 dimer, but since the comparison is with a slightly different molecule, we do not deem it to be significant. Even more reassuring is the ability of the smaller, less expensive 3-21G$^{(*)}$ basis set to reproduce the 6-31G* geometries of these systems.

Weakly bound donor–acceptor complexes such as those considered here are not necessarily well described with Hartree–Fock models.[15] In order to assess the effects of including electron correlation in the theoretical model on the structures of aluminum complexes, we compared the HF/3-21G$^{(*)}$, HF/6-31G*, HF/6-31+G*, and MP2/6-31G* optimized geometries of $H_3Al\cdots NH_3$, $Cl_3Al\cdots NH_3$, and $H_3Al\cdots H_2C{=}CH_2$ (Table III). The Hartree–Fock structures for these three complexes are all rather similar. Including additional diffuse functions in the description for the two ammonia complexes had virtually no effect on the predicted structures (the average deviation in bond lengths from 6-31G* values is less than 0.002 Å and for bond angles less than 0.1°). The best Hartree–Fock and MP2 structures for these systems do not differ appreciably either (bond lengths change by 0.01 Å or less). The Hartree–Fock prediction of the known AlN distance in $Cl_3Al\cdots NH_3$ is actually slightly closer to the experimental value than that from MP2; however, both lengths are within 0.04 Å of the measured length.

The AlC bond distance in the alane–ethylene complex is apparently quite sensitive to the computational model used. At HF/6-31G* it is nearly 0.04 Å longer than at 3-21G$^{(*)}$, while addition of diffuse functions to the basis results in a lengthening of more than 0.1 Å. Not unexpectedly, then, including electron correlation in the model significantly alters the predicted structures for the AlH_3 complex of ethylene. The CC bond length is nearly 0.02 Å longer at MP2/6-31G* than at the Hartree–Fock level. This is not surprising, given that the shortening of the AlC distance is expected to lead to increased donation from the CC π-bond into the empty aluminum p orbital and subsequent weakening of the CC bond.

This limited exploration would suggest that neither the Hartree–Fock nor the MP2 model will yield particularly good descriptions of donor–acceptor bond lengths. Our work and that of others[15] suggest that these distances will be long compared to their experimental values. It appears, then, that accurate assessments of the strength of π-complexation will require post-Hartree–Fock techniques and that even near-limiting Hartree–Fock structures can only provide upper bounds to the intermolecular separations.

Bearing in mind the results discussed above, we proceeded to compute Hartree–Fock structures for ethylene complexes of AlR_nCl_{3-n} (R = H, CH_3). These data are collected in Table IV. Again the 3-21G$^{(*)}$ and 6-31G* structures are nearly the same for both the AlH_3 and $AlCl_3$ complexes. As a result, we used the 3-21G$^{(*)}$ basis set for all further Hartree–Fock calculations. All the complexes

---

(9) Binkley, J. S.; Frisch, M.; Krishnan, R.; DeFrees, D. J.; Schlegel, H. B.; Whiteside, R.; Fluder, E.; Seeger, R.; Pople, J. A. "GAUSSIAN 82"; Carnegie-Mellon University: Pittsburgh, PA, 1982.

(10) (a) First-row elements: Binkley, J. S.; Pople, J. A.; Hehre, W. J. *J. Am. Chem. Soc.* **1980**, *102*, 939. (b) Second-row elements: Pietro, W. J.; Francl, M. M.; Hehre, W. J.; DeFrees, D. J.; Pople, J. A.; Binkley, J. S. *J. Am. Chem. Soc.* **1982**, *104*, 5039.

(11) (a) First-row elements: Hahriharan, P. C.; Pople, J. A. *Theor. Chim. Acta* **1973**, *28*, 213. (b) Second-row elements: Francl, M. M.; Pietro, W. J.; Hehre, W. J.; Binkley, J. S.; DeFrees, D. J.; Pople, J. A.; Gordon, M. S. *J. Chem. Phys.* **1982**, *77*, 3654.

(12) Frisch, M. J.; Pople, J. A.; Binkley, J. S. *J. Phys. Chem.* **1984**, *80*, 3265.

(13) Fisher, A.; Peters, N.; Haydock, K.; Poeltl, H. A.; Francl, M. M.; Jackson, N.; Lim, K.-T. Unpublished code.

(14) Jorgensen, W. L. Quantum Chemistry Program Exchange; Indiana University: Bloomington, IN; Program 340. Seida, P. R.; Francl, M. M. "MOPC", submitted to the Quantum Chemistry Program Exchange.

(15) Hehre, W. J.; Radom, L.; Schleyer, P. v. R.; Pople, J. A. *Ab Initio Molecular Orbital Theory*; Wiley: New York, 1986.

Table III. Comparison of Selected Parameters from Hartree–Fock and Post-Hartree–Fock Structures of Aluminum Lewis Acid–Lewis Base Complexes

molecule	pt group	param[a]	HF/3-21G$^{(*)}$	HF/6-31G*	HF/6-31 + G*	MP2/6-31G*	expt
$H_3Al\cdots NH_3$	C_{3v}	r(AlH)	1.608	1.603	1.602	1.606	
		∠(HAlH)	116.8	117.3	117.4	117.4	
		r(NH)	1.011	1.005	1.005	1.020	
		∠(HNH)	109.7	107.8	107.7	107.5	
		r(AlN)	2.045	2.095	2.099	2.083	
$Cl_3Al\cdots NH_3$[b]	C_{3v}	r(AlCl)	2.121	2.122	2.122	2.113	2.100
		∠(ClAlCl)	116.1	116.3	116.3	116.5	116.4
		r(NH)	1.014	1.007	1.008	1.023	
		∠(HNH)	109.2	107.6	107.5	107.5	
		r(AlN)	1.988	2.025	2.020	2.030	1.996
$H_3Al\cdots H_2C{=}CH_2$	C_s[c]	r(AlH)	1.594	1.591	1.602	1.595	
		∠(HAlH)	119.1	119.5	119.4	119.0	
		r(CC)	1.328	1.329	1.333	1.348	
		r(AlC)[d]	2.699	2.737	2.873	2.564	

[a] Bond lengths are in angstroms and bond angles in degrees. Complete structures and total energies are given in the supplementary material. [b] See ref c of Table I for experimental structure. [c] Structure confirmed as a minimum on HF/6-31G* potential energy surface by normal-mode analysis. Symmetry constrained to C_s for MP2/6-31G* optimization. [d] Average value.

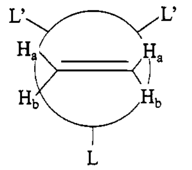

Figure 1. Newman projection down the AlL_3 C_3 axis showing the optimal conformation for bound ethylene.

exhibit the pyramidalization at the aluminum and the vinylic carbons expected to be concomitant with the shift from formal sp^2 to sp^3 hybridization. The ethylene–trichloroaluminum complex appears to be the most tightly bound, which is not unexpected since $AlCl_3$ is the strongest Lewis acid in the series considered here. The CC bond length in this molecule is nearly 0.02 Å longer than in free ethylene at the 3-21G$^{(*)}$ level. Significant pyramidalization at aluminum is also observed; the chlorine substituents are bent between 6 and 12° out of the plane.

That both $Al(CH_3)_3$ and AlH_3 are significantly weaker Lewis acids than $AlCl_3$ is evident from the structures of the corresponding ethylene complexes. Changes in the CC bond lengths are less pronounced (0.007 and 0.011 Å, respectively) than in the trichloroaluminum complex, and the alkyl substituents are bent no more than 7° out of plane. The interaction between the CC π-bond and the aluminum appears to be much stronger in the AlH_3 complex than in the trimethyl analogue; the AlC distance is more than 0.3 Å longer in the latter. In contrast, the AlC distance in only 0.1 Å longer in $AlH_3\cdots H_2C{=}CH_2$ than in $AlCl_3\cdots H_2C{=}CH_2$. Orbital energies suggest that both AlH_3 and $Al(CH_3)_3$ will have similar Lewis acidities. The LUMO energies[16] are +0.335 and +0.329 hartree for $Al(CH_3)_3$ and AlH_3, respectively. Compare these with that for $AlCl_3$, +0.221 hartree. We thus attribute the fragility of the π-complex with trimethylaluminum to steric effects. Specifically, the interaction between the vinylic and alkyl protons, i.e., F-strain,[17] appears to be the dominant factor. The preferred conformation of all these complexes (as predicted at HF/3-21G$^{(*)}$ and HF/6-31G*) is shown in Figure 1. F-strain is expected to be minimized in this conformation. In the complex with AlH_3, the hydrogens above the ligands (H_a) are bent 5° further back than those staggering the remaining ligand (H_b). The much longer aluminum–carbon distance observed upon substitution with the bulkier methyl groups relieves this strain, as evidenced by the complete lack of pyramidalization at the sp^2 carbons. For comparison, the "eclipsing" vinylic protons in the tightly bound $AlCl_3$ complex are pushed back by almost 7°.

Structures of ethylene complexes with aluminum alkyl halides ($AlClMe_2$ and $AlCl_2Me$) are similar to those of the trichloro and trimethyl complexes. In $AlCl_2Me$, the average AlC distance is 0.16 Å longer than that of $AlCl_3$. A further lengthening of 0.14 Å is observed upon exchange of a second chlorine for methyl. The trends parallel the known Lewis acidities of the aluminum monomers, i.e. $AlCl_3 > AlRCl_2 > AlR_2Cl > AlR_3$. They are also in accord with the observation that replacement of R with Cl retards the carbalumination process.

The AlH_3–propene complex is qualitatively very similar to the corresponding ethylene complex. The average AlC distance at the HF/3-21G$^{(*)}$ level is slightly shorter, 2.692 Å in the former compared to 2.699 Å in the latter. The AlH_3 fragment is pyramidalized by about 5°. The propene fragment is also nearly planar. The hydrogens are bent away from AlH_3 by about 5°, and the more sterically demanding methyl group is bent by about 15°. The CC double bond is virtually parallel to the plane of the alane hydrogens; it is tipped by about 10° such that the α-carbon is slightly further from the aluminum. The conformation of the propene relative to the alane is much the same as that shown for ethylene in Figure 1. The AlH bond no longer exactly bisects C=C; it is twisted roughly 15° off the perpendicular. The CC double bond is longer than that in free propene at the same level, 1.331 Å compared to 1.316 Å.[15] The CC single bond is also slightly elongated relative to the length in the isolated molecule. This is not unexpected, since the hyperconjugative effect that shortens the propene CC single bond relative to "normal" bonds will be reduced due to the π-withdrawing effect of the alane fragment.

B. Bonding. A qualitative MO scheme describing the binding of $H_2C{=}CH_2$ to AlH_3 is shown in Figure 2. The bonding is classic Lewis acid–base and is expected to be quite weak due to the large difference in energies between the LUMO on the alane and the HOMO on ethylene. The MO plot in Figure 3 depicts the ethylene–aluminum bonding orbital. Note the minimal contribution of the aluminum p orbital to the surface, a further indication of the weakness of the interaction. (The mixing of hydrogen 1s into this MO is a result of the pyramidalization at

---

(16) Orbital energies from HF/3-21G$^{(*)}$//HF/3-21G$^{(*)}$ calculations.

(17) Brown, H. C.; Davidson, N. *J. Am. Chem. Soc.* **1942**, *64*, 316. Buhr, Muller, G. E. *Chem. Ber.* **1955**, *88*, 251.

Table IV. Selected Parameters from Hartree–Fock Optimized Structures for AlL_3–$H_2C{=}CHR$ Complexes

AlL_3	R	param[a]	HF/3-21G(*)	HF/6-31G*
AlH_3[b]	H	r(AlH)	1.594	1.591
		r(AlH′)	1.594	1.590
		∠(H′AlX)	96.7	96.4
		∠(HAlX)	94.9	94.6
		r(CC)	1.326	1.328
		∠(HCH)	116.7	116.8
		r(AlC)[c]	2.699	2.737
$Al(CH_3)_3$[b]	H	$r(\mathrm{AlC_{Me}})$	1.990	1.989
		$r(\mathrm{AlC_{Me}'})$	1.988	1.986
		$\angle(\mathrm{C'_{Me}AlX})$	95.2	94.8
		$\angle(\mathrm{C_{Me}AlX})$	94.9	95.3
		r(CC)	1.322	1.323
		∠(HCH)	116.4	116.5
		r(AlC)[c]	3.023	3.092
$AlCl_3$[b]	H	r(AlCl)	2.109	2.112
		r(AlCl′)	2.105	2.108
		∠(Cl′AlCl′)		117.8
		∠(ClAlCl′)		116.3
		r(CC)	1.333	1.333
		∠(HCH)	116.9	117.0
		r(AlC)[c]	2.591	2.628
$AlCl_2CH_3$	H	r(AlCl)	2.125	
		$r(\mathrm{AlC_{Me}})$	1.958	
		$\angle(\mathrm{C_{Me}AlC_{Me}})$	126.3	
		r(CC)	1.323	
		∠(HCH)	116.6	
		r(AlC)[c]	2.747	
$AlCl(CH_3)_2$	H	r(AlCl)	2.143	
		$r(\mathrm{AlC_{Me}})$	1.972	
		∠(ClAlCl)	124.4	
		r(CC)	1.325	
		∠(HCH)	116.5	
		r(AlC)[c]	2.885	
AlH_3	CH_3	r(AlH)	1.594	
		r(AlH′)[c]	1.594	
		∠(H′AlH′)	118.5	
		∠(HAlH′)[c]	118.6	
		r(C=C)	1.331	
		r(C—C)	1.507	
		∠(HCH)	116.8	
		$\angle(\mathrm{C_{Me}CH})$	116.2	
		r(AlC)[c]	2.692	

[a] Bond lengths are in angstroms and angles in degrees. Complete structures and total energies are given in the supplementary material. [b] The L and L′ notations refer to the Newman projection

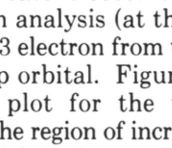

X is defined as the point of intersection of the CC bond axis and the plane bisecting the L′AlL′ angle. In symmetrically bound alkenes, this is the midpoint of the bond. [c] Average value.

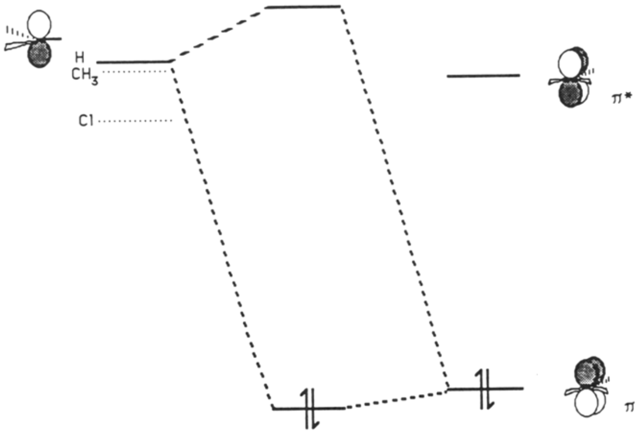

Figure 2. Qualitative MO interaction diagram for ethylene with the AlL_3 fragment. The relative energies of the empty p orbital on the trihydride, trimethyl and trichloro fragments are to scale.

aluminum, in which case it becomes symmetry allowed.) Mulliken population analysis (at the HF/3-21G(*) level) indicates a shift of 0.3 electron from the ethylene fragment into the aluminum p orbital. Figure 4 shows the charge density difference plot for the trimethylaluminum–ethylene complex. The region of increased density between the two carbons, which is characteristic of the π-bond, is relatively symmetrical about the CC bond axis, suggesting that the integrity of the bond is not significantly affected by complexation. The above evidence supports the structural data in suggesting that the ethylene complexes are weakly bound.

C. Binding Energies. Calculated energies for binding of ethylene to $R_nCl_{3-n}Al$ and dimerization of $R_nCl_{3-n}Al$ are collected in Table V. While not a great deal of comparison can be drawn with experiment, it is clear that the HF/3-21G(*) level is inadequate to the task of predicting absolute reaction energies for these systems. The enthalpy of dimerization of $Al(CH_3)_3$ is known to be −19 kcal/mol (at 298 K);[18] HF/3-21G(*) underestimates the reaction energy by more than 13 kcal/mol. The model yields somewhat better results for the dimerization of $AlCl_3$. In this case, HF/3-21G(*) predicts a reaction energy of −25 kcal/mol, compared to the experimental value of −30 kcal/mol (at 0 K).[19] The order of the relative stabilities of the two dimers $(AlCl_3)_2$ and $[Al(CH_3)_3]_2$ is correctly predicted. Using the larger 6-31G* basis set does not improve the comparison with experiment. In fact, the energy of dimerization of trimethylaluminum is predicted to be slightly *positive* at this level. The computed energy of dimerization for AlH_3, corrected for the zero-point energy and to 298 K,[20] is −24 kcal/mol at the HF/6-31G* level and −27 kcal/mol at the MP2/6-31G*//HF/6-31G* level.

No experimental values are available for the energy of complexation of $H_2C{=}CH_2$ to $R_nCl_{3-n}Al$. Dolzine and Oliver have estimated that olefin–alane complexes are bound by between 2 and 7 kcal/mol.[2] Our data are in accord with their estimates; at the HF/3-21G(*) level complexation energies are computed to range from 6 to 14 kcal/mol. Given the difficulties discussed above, this agreement may be fortuitous. HF/6-31G* energies are also found to be within the range suggested by Dolzine and Oliver for both the AlH_3 and $AlMe_3$ complexes. Single points at the MP2/6-31G*//HF/6-31G* level predict these complexes to be roughly 2–3 kcal/mol more stable than the HF/6-31G* model. Interestingly, though the optimized structure for the AlH_3 complex changes significantly when the MP2/6-31G* model is used, the complexation energy is relatively insensitive. At the MP2/6-31G*//HF/6-31G* level, complexation is favored by 11 kcal/mol, while at the MP2/6-31G*//MP2/6-31G* level, it is favored by 12 kcal/mol. Addition of diffuse functions to the basis set also does not appear to have a significant impact on the predicted binding energy of ethylene to alane. This is not surprising in view of the lack of effect these functions have on the computed structures. In all cases, however, the relative stabilities do reflect both the known trends in

---

(18) Smith, M. B. *J. Organomet. Chem.* **1974**, *70*, 13.

(19) Stull, D. R.; Prophet, J. *JANAF Thermochemical Tables*, 2nd ed.; NSRDS-NBS 37; National Bureau of Standards: Washington, DC, 1971.

(20) See Table V, ref *b*, for details.

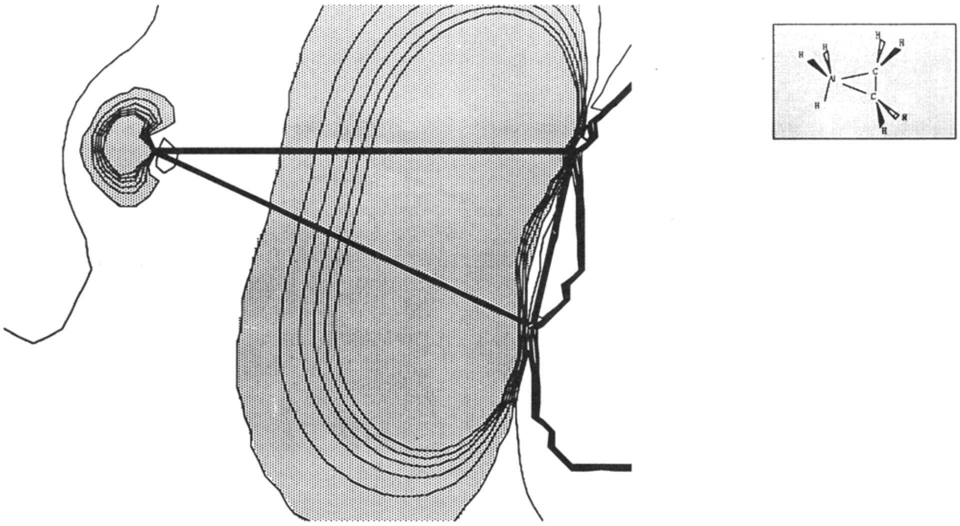

Figure 3. Cross section of the aluminum–ethylene π-bonding orbital in $AlH_3\cdots C_2H_4$ taken in the AlCC plane. White regions indicate regions of positive phase; shading indicates areas of negative phase.

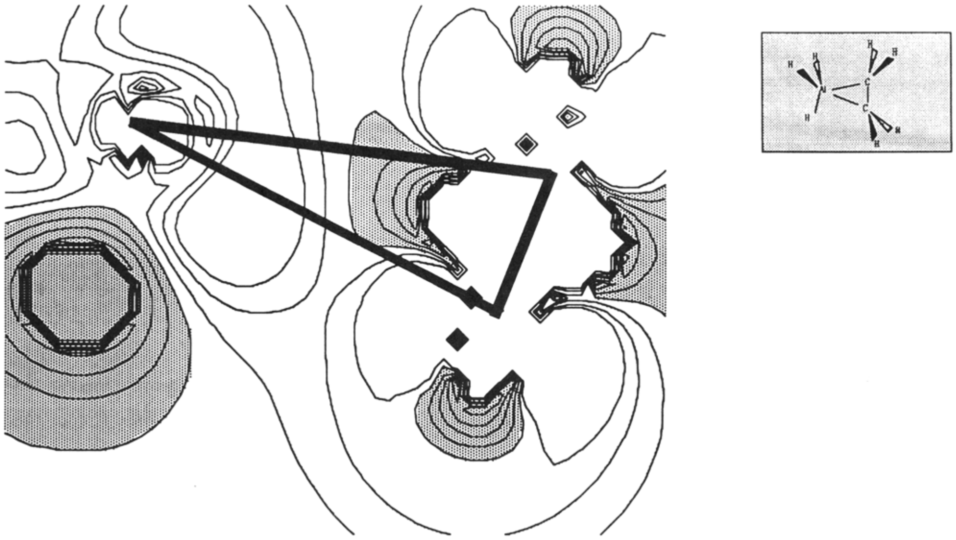

Figure 4. Charge density difference plot of the AlH_3 complex with ethylene in the AlCC plane. Light areas indicate an increase in electron density relative to that of the separated spherical atoms, while shaded regions indicate a loss of density.

Table V. Reaction Energies[a]

AlL_nR_{3-n}	reacn	HF/3-21G$^{(*)}$// HF/3-21G$^{(*)}$	HF/6-31G*// HF/6-31G*	MP2/6-31G*// HF/6-31G*	MP2/6-311+G*// HF/6-31G*
AlH_3[b]	dimerizn	−30 (−27)	−27	−30	−33
	complexn	−9.8 (−7.2)	−7.8	−11	−10
$AlMe_3$	dimerizn	−5.8	0.6		
	complexn	−5.7	−4.2	−7.0	
$AlMe_2Cl$	complexn	−6.8			
$AlMeCl_2$	complexn	−9.2			
$AlCl_3$	dimerizn	−25	−18		
	complexn	−14	−10		

[a] Reaction energies in kcal mol^{-1}. [b] Values in parentheses corrected for the zero-point energy and to 298 K as follows: $E_{\text{zero point}} = {}^1/_2\sum h\nu_i$; $H(298) = H_{\text{vib}} + H_{\text{rot}} + H_{\text{trans}}$; $H_{\text{vib}} = N\sum h\nu_i/[\exp(h\nu_i/kT) - 1] + RT$; $H_{\text{rot}} = {}^3/_2RT$; $H_{\text{trans}} = {}^3/_2RT$. Vibrational modes less than 400 cm^{-1} were treated as rotations in the calculation of H_{vib}. HF/3-21G$^{(*)}$ normal-mode frequencies were used.

Lewis acidity and the AlC distances computed in this work.

D. Binding Orientation. There is virtually no inherent *electronic* preference for the orientation of ethylene bound to AlL_3, as the qualitative MO scheme in Figure 2 would suggest. The barrier to "rotation" of the olefin about the pseudo-C_3 axis on top of an L_3Al fragment is much less than 1 kcal/mol. At the HF/3-21G$^{(*)}$ level for L = H, it is only 0.1 kcal/mol! Similarly, the rigid barrier to rotation of propene bound to AlH_3 is 0.7 kcal/mol. Substitution at aluminum with methyl groups is expected to raise the barrier substantially. We modeled this complex using the $AlMe_3$ parameters from the trimethylaluminum–ethylene complex and the propene parameters from the alane–propene complex. The AlC distances were fixed at those from the trimethylaluminum–ethylene structure. At the HF/3-21G$^{(*)}$ level, this crude model suggests that the barrier to rotation will be approximately 2 kcal/mol.

In order to exert substantial control over the stereo- and regiochemistry of polymerization and carbalumination, these results suggest it would be necessary to use rather bulky ligands on the aluminum center. This would have the dual effect of controlling the binding orientation and destabilizing the aluminum dimer, though care must be taken that not so much steric bulk is introduced into the systems that the binding of substrate becomes unfavorable as well. Comparisons of the dimerization and complexation reaction energies of AlH_3 and $Al(CH_3)_3$ suggest that the former reaction is likely to be far more sensitive to steric factors. Note especially that the parent complexes have similar Lewis acidities. Experimental work is in accord with these results.[21]

Conclusions

We find that complexes of simple alkenes with $R_nCl_{3-n}Al$ are stable intermediates. Binding in most cases is predicted to be somewhat less favorable than dimerization, though these results should be viewed with caution. Binding does not significantly affect the C=C bond in ethylene, as evidenced by CC bond distances and CC stretching frequencies. The systems exhibit true olefin-metal complexation. The trends in complex stability follow the trends in the Lewis acidities of the parent $R_nCl_{3-n}Al$ fragments, i.e. $AlCl_3 > AlCl_2CH_3 > AlCl(CH_3)_2 > Al(CH_3)_3$. To first order, there is no electronic preference for orientation of an alkene to aluminum; steric effects are expected to be the controlling factor in determining the regiochemistry of addition. Work is currently in progress in this group to characterize the transition structures linking the intermediates described here and the related insertion products.

Acknowledgment. We appreciate the support of the Academic Computing Centers of Bryn Mawr College and Haverford College. P.R.S. and Y.-M.C. thank Bryn Mawr College and the Charles A. Dana Foundation for fellowship support. M.M.F. thanks Dr. Kerwin Dobbs and John Freeman for many helpful discussions.

Registry No. AlH_3, 7784-21-6; $Al(CH_3)_3$, 75-24-1; $AlCl_3$, 7446-70-0; $AlCl(CH_3)_2$, 1184-58-3; $AlCl_2CH_3$, 917-65-7; $(AlH_3)_2$, 12004-30-7; $[Al(CH_3)_3]_2$, 15632-54-9; $(AlCl_3)_2$, 13845-12-0; $H_3Al{\cdots}NH_3$, 27710-55-0; $Cl_3Al{\cdots}NH_3$, 15550-69-3; $H_3Al{\cdots}H_2C{=}CH_2$, 128660-20-8; $Al(CH_3)_3{\cdots}H_2C{=}CH_2$, 128660-21-9; $AlCl_3{\cdots}H_2C{=}CH_2$, 12175-82-5; $AlCl_2CH_3{\cdots}H_2C{=}CH_2$, 128683-52-3; $AlCl(CH_3)_2{\cdots}H_2C{=}CH_2$, 128660-22-0; $AlH_3{\cdots}H_2C{=}CHCH_3$, 128660-23-1.

Supplementary Material Available: Tables of full Cartesian coordinates and total energies for all optimized structures included in this paper (7 pages). Ordering information is given on any current masthead page.

---

[21] Eisch, J. J.; Kaska, W. C. *J. Am. Chem. Soc.* **1966**, *88*, 2213. Eisch, J. J.; Amtmann, R. *J. Org. Chem.* **1972**, *37*, 3420.

Synthesis of Iron Carbonyl Clusters with Trigonal-Bipyramidal E_2Fe_3 Cores (E = Ge, Si). Crystal Structures of $(\mu_3\text{-GeEt})_2Fe_3(CO)_9$, $[\mu_3\text{-Ge}\{Fe(CO)_2Cp\}]_2Fe_3(CO)_9$, and $[\mu_3\text{-Si}\{Fe(CO)_2Cp\}]_2Fe_3(CO)_9$

Skelte G. Anema, Kenneth M. Mackay,* Brian K. Nicholson,* and Martin Van Tiel

School of Science and Technology, University of Waikato, Hamilton, New Zealand

Received August 8, 1989

The reaction of $RGeH_3$ with $Fe_3(CO)_{12}$ at 50 °C gives low-to-moderate yields of the trigonal-bipyramidal clusters $(\mu_3\text{-GeR})_2Fe_3(CO)_9$ (**3**) together with complexes tentatively identified as $(\mu\text{-GeRH})_2Fe_2(CO)_7$ and $(\mu\text{-GeRH})_3Fe_2(CO)_6$. A superior route to clusters **3** is from $RGeH_3$ and $Fe(CO)_5$ at 140 °C. The corresponding reactions with silanes $RSiH_3$ appear to give similar products, but the lack of stability precluded complete characterization. The stable Si_2Fe_3-core cluster $[\mu_3\text{-Si}\{Fe(CO)_2Cp\}]_2Fe_3(CO)_9$ (**5a**) can be prepared in good yield by reacting SiH_4 with $Fe(CO)_5$ and $[Fe(CO)_2Cp]_2$ at 150 °C; the corresponding Ge analogue **5b** is similarly available from GeH_4. X-ray crystal structures are reported for cluster **3** (R = Et; $C_{13}H_{10}Fe_3Ge_2O_9$, $a = 9.341$ (2) Å, $b = 15.264$ (4) Å, $c = 14.216$ (3) Å, $\beta = 91.22$ (2)°, $P2_1/n$, $Z = 4$), for **5a** ($C_{23}H_{10}Fe_5Si_2O_{13}$, $a = 10.020$ (8) Å, $b = 9.914$ (6) Å, $c = 28.07$ (2) Å, $\beta = 92.68$ (7)°, $P2_1/n$, $Z = 4$), and for **5b** ($C_{23}H_{10}Fe_5Ge_2O_{13}$, $a = 10.125$ (3) Å, $b = 10.024$ (3) Å, $c = 28.308$ (9) Å, $\beta = 92.53$ (3)°, $P2_1/n$, $Z = 4$). The E_2M_3 cores are slightly irregular trigonal bipyramids with Ge–Fe ranging from 2.302 to 2.336 Å and Fe–Fe = 2.721–2.742 Å in **3**; in **5a**, Si–Fe = 2.294–2.324 Å (distinctly longer than the external Si–Fe value of 2.251 Å) and Fe–Fe is 2.654–2.687 Å, while in **5b** Ge–Fe = 2.365–2.391 Å (external Ge–Fe = 2.318 Å) and Fe–Fe = 2.717–2.742 Å.

Introduction

Clusters containing a *closo*-E_2M_3 core, where E is a main-group element and M is a transition metal, are relatively rare.[1] In 1988, Whitmire[2] listed only nine examples, of which five were P_2Fe_3 species. Crystallographically established examples where E is a group 14 element are limited to the long-known[3] $[\mu_3\text{-SnCl}_3]_2Pt_3(C_8H_{12})_3$, the sparsely described[4] $[\mu_3\text{-Sn}\{Fe(CO)_2Cp\}]_2Fe_3(CO)_9$ (**5c**), and three complexes not in Whitmire's review,[2] $(\mu_3\text{-CF})_2Fe_3(CO)_9$[5] and the pair $[\mu_3\text{-E}\{Re(CO)_5\}]_2Fe_3(CO)_9$ (E = Sn,[6]

---

[1] Herrmann, W. A. *Angew. Chem., Int. Ed. Engl.* **1986**, *25*, 56.

[2] Whitmire, K. H. *J. Coord. Chem.* **1988**, *17*, 95.

[3] Guggenberger, L. J. *J. Chem. Soc., Chem. Commun.* **1968**, 512.

[4] McNeese, J. T.; Wreford, S.; Tipton, L. D.; Bau, R. *J. Chem. Soc., Chem. Commun.* **1977**, 390.

[5] Lentz, D.; Brudgam, I.; Hartl, H. *Angew. Chem., Int. Ed. Engl.* **1985**, *24*, 119.